Qualitative and Numerical Simulation of a Time-Fractional SEIR Mpox Model Arising in Population Epidemiology

Gaurav Saini[*], Bappa Ghosh[†‡], Sunita Chand[§], Jugal Mohapatra[¶]

Abstract

Epidemiological modeling is vital in understanding disease dynamics and guiding public health interventions. This study presents a time-fractional SEIR model to describe the transmission dynamics of Mpox, incorporating memory effects via the fractional derivative. We perform an extensive qualitative investigation, proving that there is a unique solution and that the solutions are Hyers-Ulam stable. To approximate the model numerically, we implement the L1 finite difference scheme for the Caputo derivative and solve the resulting nonlinear system using the Newton-Raphson technique. A detailed error analysis is provided, demonstrating that the scheme achieves algebraic convergence. Comparative results with the Fractional Modified Euler method (FMEM) confirm the superior accuracy and stability of the proposed approach. Numerical simulations under biologically relevant parameters illustrate the impact of the non-integer order and vaccination rate on disease progression. The study underscores the effectiveness of fractional order models in capturing epidemic memory effects and positions the L1 scheme as a robust numerical tool for simulating such dynamics.

Keywords: Mpox virus, Time-fractional SEIR model, L1 scheme.

MSC Code : 26A33, 37M05, 92D25, 65L05.

[*]Center for Data Science, Department of Computer Science and Engineering, Siksha 'O' Anusandhan (Deemed to be University), India

[†]Center for Artificial Intelligence and Machine Learning, Department of Computer Science and Engineering, Siksha 'O' Anusandhan (Deemed to be University), India

[‡]Corresponding author. Email-bg12.ghosh@gmail.com

[§]Department of Mathematics, Siksha 'O' Anusandhan (Deemed to be University), India

[¶]Department of Mathematics, National Institute of Technology, Rourkela, India.

1 Introduction

Population dynamics models are mathematical frameworks that describe changes in population sizes over time, influenced by various biological and environmental factors. These models are particularly important in understanding the spread of infectious diseases and in designing effective control strategies across disciplines such as ecology, epidemiology, and resource management. Mpox, often known as monkeypox, is a re-emerging zoonotic infection caused by the Monkeypox virus, which is a member of the Poxviridae family's Orthopoxvirus genus. First identified in 1958 in monkeys and subsequently in humans in the Democratic Republic of the Congo in 1970, Mpox has garnered renewed global attention due to recent outbreaks outside endemic regions. The virus mainly spreads to humans through direct interaction with infected animals or individuals, involving exposure to bodily fluids, respiratory droplets, or contaminated objects [3]. Although symptoms are similar to smallpox fever, rash, lymphadenopathy Mpox is generally less severe but still poses a significant public health concern, especially in immunocompromised individuals. The increasing frequency of outbreaks and the potential for human-to-human transmission emphasize the need for accurate mathematical models to understand the disease dynamics and evaluate the effectiveness of intervention strategies such as isolation, vaccination, and behavioral change. The dynamics of Mpox virus transmission can be described using a classical SEIR-type model, where the total population is stratified into four epidemiological classes: susceptible ($\widehat{S}$), exposed ($\widehat{E}$), infectious ($\widehat{I}$), and recovered ($\widehat{R}$). The classical (integer-order) model for $t > 0$ is formulated as [1]

$$\begin{cases} \dfrac{d\widehat{S}(t)}{dt} = \Lambda - \beta \widehat{S}(t)\widehat{I}(t) - (\nu + \mu)\, \widehat{S}(t), \\ \dfrac{d\widehat{E}(t)}{dt} = \beta \widehat{S}(t)\widehat{I}(t) - (\gamma + \mu)\, \widehat{E}(t), \\ \dfrac{d\widehat{I}(t)}{dt} = \gamma \widehat{E}(t) - (\alpha + \sigma + \mu)\, \widehat{I}(t), \\ \dfrac{d\widehat{R}(t)}{dt} = \nu \widehat{S}(t) + \alpha \widehat{I}(t) - \mu\, \widehat{R}(t), \end{cases}$$

subject to the conditions $\widehat{S}(0) = \widehat{S}_0, \quad \widehat{E}(0) = \widehat{E}_0, \quad \widehat{I}(0) = \widehat{I}_0, \quad \widehat{R}(0) = \widehat{R}_0$.

Fractional calculus is a natural extension of classical calculus that allows derivatives and integrals to be defined for arbitrary (non-integer) orders. This extension introduces memory and hereditary properties into dynamic systems, which are especially important for accurately describing real-world phenomena. Fractional-order differential equations (FDEs) have found wide application in modeling complex systems such as viscoelastic materials [27], anomalous diffusion [15], financial systems [6], and population dynamics [29, 7]. For an in-depth treatment of fractional calculus, see [10, 16, 19, 21]. Traditional integer-order models often fail to capture long-range dependencies and memory effects observed in real-world data. Despite their increased mathematical complexity and computational cost, fractional-order models offer enhanced flexibility and accuracy in simulating disease spread and evaluating

Symbol	Description
$\widehat{S}(t)$	Number of susceptible individuals
$\widehat{E}(t)$	Number of exposed individuals
$\widehat{I}(t)$	Number of infectious individuals
$\widehat{R}(t)$	Number of recovered (or vaccinated) individuals
Λ	Recruitment rate into the susceptible class
β	Rate of transmission (susceptible to exposed)
ν	Vaccination rate of susceptible individuals
γ	Rate of progression from exposed to infectious
α	Recovery rate from infection
μ	Natural death rate
σ	Disease-induced death rate

Table 1: Model variables and parameters.

intervention outcomes. In this work, we study the following fractional-order Mpox model [1]

$$\begin{cases} \mathcal{D}_t^\rho \widehat{S}(t) = \Lambda - \beta \widehat{S}(t)\widehat{I}(t) - (\nu + \mu)\, \widehat{S}(t), \\ \mathcal{D}_t^\rho \widehat{E}(t) = \beta \widehat{S}(t)\widehat{I}(t) - (\gamma + \mu)\, \widehat{E}(t), \\ \mathcal{D}_t^\rho \widehat{I}(t) = \gamma \widehat{E}(t) - (\alpha + \sigma + \mu)\, \widehat{I}(t), \\ \mathcal{D}_t^\rho \widehat{R}(t) = \nu \widehat{S}(t) + \alpha \widehat{I}(t) - \mu\, \widehat{R}(t), \end{cases} \tag{1.1}$$

where $\mathcal{D}_t^\rho$ denotes the Caputo derivative of order $\rho \in (0, 1)$, defined by [19]

$$\mathcal{D}_t^\rho \phi(x) = \int_a^x \frac{(x-t)^{-\rho}\, \phi'(t)}{\Gamma(1-\rho)} dt, \qquad 0 < \rho < 1.$$

Mathematical modeling has played a pivotal role in understanding the transmission dynamics of the Mpox virus, assessing the effectiveness of public health interventions, and forecasting potential outbreak scenarios. Due to the fractional order systems nonlinear and nonlocal nature, obtaining exact analytical solutions is typically intractable. Consequently, considerable efforts have been devoted to developing numerical and semi-analytical techniques that approximate these models with high accuracy. These approaches offer valuable insights into the long-memory behavior of the disease and enable the evaluation of key parameters affecting the spread and control of Mpox.To mention a few: Peter et al. [18] investigated an arbitrary-order compartmental model of Mpox transmission using the Caputo–Fabrizio fractional derivative to incorporate memory effects. The authors established existence and uniqueness of solutions via fixed point theory and presented numerical simulations illustrating the disease dynamics for different fractional orders. In a related effort, Majee et al. [13] implemented the two-step Adams–Bashforth–Moulton method, a predictor–corrector

scheme, to integrate a Caputo-based model numerically. Their approach combined the stability of implicit updates with the simplicity of explicit predictors, enhancing both accuracy and computational performance. Batiha et al. [1] addressed a fractional SEIR model for Mpox using the Fractional Euler Method and the Modified Fractional Euler Method. Kumar et al. [11] similarly focused on Caputo-based formulations, using a finite-difference predictor–corrector algorithm to solve their system and assess transmission behavior under varying fractional orders. Further extending the analysis, Elsonbaty et al. [5] examined the numerical simulations and applied the classical fourth-order RK method to illustrate the impact of model parameters on the progression and stability of the outbreak. Paul et al. [17] adopted a Lagrangian piecewise interpolation technique to approximate solutions of a control-based Mpox system. A different perspective used by Rahman et al. [20], who reformulated their Caputo-type system as a Volterra integral equation and applied an iterative scheme to obtain solutions. Ramzan et al. [22] used the Caputo–Fabrizio fractional operator, known for its non-singular kernel, to construct a modified model of Mpox. Their numerical analysis utilized an adapted 4^{th} order RK method to handle the nonlocal behavior. Manivel et al. [14] developed a Caputo-type arbitrary-order model and solved it using the Variational Iteration Method (VIM), a semi-analytical technique based on Lagrange multipliers. Helikumi et al. [8] employed the predictor corrector method to approximate the dynamics, demonstrating the importance of memory in predicting outbreak trajectories and informing public health responses.Tunç et al. [26, 25, 2, 24] investigated the Ulam-type (Hyper-Ulam) stability of nonlinear integral and fractional integro-differential equations by employing Banach's fixed-point theorem and Bielecki norms. Their results provide new qualitative insights for Volterra, Fredholm, and delay systems, thereby enriching the existing stability theory.

Motivated by recent developments in the literature, we conduct a qualitative analysis of a time-fractional Mpox transmission model governed by a Caputo derivative of arbitrary order. The focus is placed on establishing the existence, uniqueness, and stability of its analytical solution. Furthermore, an efficient iterative finite difference scheme is developed based on the standard L1 technique to approximate the solution of the nonlinear fractional system (1.1). Theoretical results are supported by numerical experiments that validate the accuracy and effectiveness of the proposed approach. This paper is structured as follows:Section 2 is devoted to the existence and uniqueness of solutions for the fractional Mpox model. Stability analysis is carried out in Section 3. The construction of the numerical scheme using the L1 method is detailed in Section 4 with error analysis in Section 5, while Section 6 presents the results of numerical simulations. Concluding remarks and future directions are discussed in Section 7.

2 Existence and Uniqueness of Solutions

In this section, we establish the existence of solutions to the time-fractional Mpox model (1.1) by employing fixed-point theory. An equivalent integral version of the model is obtained by applying the fractional integral operator at (1.1).

$$\begin{cases} \widehat{S}(t) = \widehat{S}_0 + \displaystyle\int_0^t \frac{(t-z)^{\rho-1} F_1(z, \widehat{S}(z))}{\Gamma(\rho)}\, dz, \quad \widehat{E}(t) = \widehat{E}_0 + \int_0^t \frac{(t-z)^{\rho-1} F_2(z, \widehat{E}(z))}{\Gamma(\rho)}\, dz, \\ \widehat{I}(t) = \widehat{I}_0 + \displaystyle\int_0^t \frac{(t-z)^{\rho-1} F_3(z, \widehat{I}(z))}{\Gamma(\rho)}\, dz, \quad \widehat{R}(t) = \widehat{R}_0 + \int_0^t \frac{(t-z)^{\rho-1} F_4(z, \widehat{R}(z))}{\Gamma(\rho)}\, dz, \end{cases}$$

where $\widehat{S}_0, \widehat{E}_0, \widehat{I}_0, \widehat{R}_0$ are the initial conditions, and the nonlinear functions F_i are defined as:

$$\begin{cases} F_1(z, \widehat{S}(t)) = \Lambda - \beta \widehat{S}(t)\widehat{I}(t) - (\nu + \mu)\widehat{S}(t), \quad F_2(z, \widehat{E}(t)) = \beta \widehat{S}(t)\widehat{I}(t) - (\mu + \gamma)\widehat{E}(t), \\ F_3(z, \widehat{I}(t)) = \gamma \widehat{E}(t) - (\mu + \sigma + \alpha)\widehat{I}(t), \quad F_4(z, \widehat{R}(t)) = \nu \widehat{S}(t) + \alpha \widehat{I}(t) - \mu \widehat{R}(t). \end{cases}$$

Assumptions (C): We assume that the functions $\widehat{S}^i(z), \widehat{E}^i(z), \widehat{I}^i(z), \widehat{R}^i(z)$, for $i = 1, 2$, all belong to $L^1[0, 1]$, and $\|\widehat{S}\| \leq q_1, \quad \|\widehat{E}\| \leq q_2, \quad \|\widehat{I}\| \leq q_3, \quad \|\widehat{R}\| \leq q_4$ for some real constants $q_1, q_2, q_3, q_4 > 0$.

Theorem 2.1. *The kernel functions F_1, F_2, F_3, F_4 satisfy the Lipschitz condition under assumption (C), provided that $0 \leq \kappa_i < 1$ for all $i = 1, 2, 3, 4$.*

Proof. We first verify the Lipschitz continuity of $F_1(t, \widehat{S})$. We have,

$$\begin{aligned} \|F_1(t, \widehat{S}^1) - F_1(t, \widehat{S}^2)\| &= \|\Lambda - \beta \widehat{S}^1 \widehat{I} - (\nu + \mu)\widehat{S}^1 - (\Lambda - \beta \widehat{S}^2 \widehat{I} - (\nu + \mu)\widehat{S}^2)\| \\ &= \|\beta \widehat{I}(\widehat{S}^2 - \widehat{S}^1) + (\nu + \mu)(\widehat{S}^2 - \widehat{S}^1)\| \leq (\beta q_3 + \nu + \mu)\|\widehat{S}^2 - \widehat{S}^1\| \leq \kappa_1 \|\widehat{S}^2 - \widehat{S}^1\|, \end{aligned}$$

where $\kappa_1 = \beta q_3 + \nu + \mu$. Hence, F_1 satisfies the Lipschitz condition if $\kappa_1 < 1$. Next, for $F_2(t, \widehat{E})$, we compute,

$$\begin{aligned} \|F_2(t, \widehat{E}^1) - F_2(t, \widehat{E}^2)\| &= \|\beta \widehat{S}\widehat{I} - (\mu + \gamma)\widehat{E}^1 - (\beta \widehat{S}\widehat{I} - (\mu + \gamma)\widehat{E}^2)\| \\ &= (\mu + \gamma)\|\widehat{E}^1 - \widehat{E}^2\| = \kappa_2 \|\widehat{E}^1 - \widehat{E}^2\|, \end{aligned}$$

with $\kappa_2 = \mu + \gamma$. Thus, F_2 satisfies the Lipschitz condition if $\kappa_2 < 1$. Now, for $F_3(t, \widehat{I})$, we have,

$$\begin{aligned} \|F_3(t, \widehat{I}^1) - F_3(t, \widehat{I}^2)\| &= \|\gamma \widehat{E} - (\mu + \sigma + \alpha)\widehat{I}^1 - (\gamma \widehat{E} - (\mu + \sigma + \alpha)\widehat{I}^2)\| \\ &= (\mu + \sigma + \alpha)\|\widehat{I}^1 - \widehat{I}^2\| = \kappa_3 \|\widehat{I}^1 - \widehat{I}^2\|, \end{aligned}$$

where $\kappa_3 = \mu + \sigma + \alpha$. Thus, F_3 is Lipschitz continuous if $\kappa_3 < 1$. Finally, for $F_4(t, \widehat{R})$

$$\|F_4(t, \widehat{R}^1) - F_4(t, \widehat{R}^2)\| = \|\nu \widehat{S} + \alpha \widehat{I} - \mu \widehat{R}^1 - (\nu \widehat{S} + \alpha \widehat{I} - \mu \widehat{R}^2)\| = \mu \|\widehat{R}^1 - \widehat{R}^2\| = \kappa_4 \|\widehat{R}^1 - \widehat{R}^2\|,$$

where $\kappa_4 = \mu$. So, F_4 satisfies the Lipschitz condition if $\kappa_4 < 1$. Therefore, all F_i $(i = 1, 2, 3, 4)$ satisfy Lipschitz continuity under the condition $0 \leq \kappa_i < 1$, which completes the proof. □

Now, we reformulate the fractional-order Mpox model using the nonlinear kernels F_i introduced earlier. we assume without loss of generality that the initial conditions are shifted to zero by a standard translation of variables. That is, for given initial data $\widehat{S}(0) = \widehat{S}_0$, $\widehat{E}(0) = \widehat{E}_0$, $\widehat{I}(0) = \widehat{I}_0$, and $\widehat{R}(0) = \widehat{R}_0$, one may consider the transformed variables $\widehat{X}(t) - \widehat{X}_0$.

$$\begin{cases} \widehat{S}(t) = \displaystyle\int_0^t \frac{(t-z)^{\rho-1} F_1(z, \widehat{S}(z))}{\Gamma(\rho)}\, dz, \quad \widehat{E}(t) = \int_0^t \frac{(t-z)^{\rho-1} F_2(z, \widehat{E}(z))}{\Gamma(\rho)}\, dz, \\ \widehat{I}(t) = \displaystyle\int_0^t \frac{(t-z)^{\rho-1} F_3(z, \widehat{I}(z))}{\Gamma(\rho)}\, dz, \quad \widehat{R}(t) = \int_0^t \frac{(t-z)^{\rho-1} F_4(z, \widehat{R}(z))}{\Gamma(\rho)}\, dz, \end{cases} \tag{2.1}$$

We define a recursive sequence of functions to construct an approximate solution iteratively

$$\begin{cases} \widehat{S}_k(t) = \displaystyle\int_0^t \frac{(t-z)^{\rho-1} F_1(z, \widehat{S}_{k-1}(z))}{\Gamma(\rho)}\, dz, \quad \widehat{E}_k(t) = \int_0^t \frac{(t-z)^{\rho-1} F_2(z, \widehat{E}_{k-1}(z))}{\Gamma(\rho)}\, dz, \\ \widehat{I}_k(t) = \displaystyle\int_0^t \frac{(t-z)^{\rho-1} F_3(z, \widehat{I}_{k-1}(z))}{\Gamma(\rho)}\, dz, \quad \widehat{R}_k(t) = \int_0^t \frac{(t-z)^{\rho-1} F_4(z, \widehat{R}_{k-1}(z))}{\Gamma(\rho)}\, dz, \end{cases}$$

where the sequence $\{(\widehat{S}_k, \widehat{E}_k, \widehat{I}_k, \widehat{R}_k)\}_{k=0}^{\infty}$ is constructed with initial approximations set to zero or any suitable function in $L^1[0,1]$. Convergence of this sequence under suitable Lipschitz assumptions guarantees the existence of a unique solution.

Theorem 2.2. *The time-fractional Mpox model* (1.1) *admits at least one solution if the following condition holds* $\sigma = \max\{\kappa_1, \kappa_2, \kappa_3, \kappa_4\} < 1$.

Proof. Let $D\widehat{X}_{k+1}(t) = \widehat{X}_{k+1}(t) - \widehat{X}_k(t)$ denote the difference between two successive Picard iterates. We begin by estimating the difference between two successive approximations of the susceptible population

$$\begin{aligned} \|D\widehat{S}_{k+1}(t)\| = \left\|\widehat{S}_{k+1}(t) - \widehat{S}_k(t)\right\| &= \left\| \int_0^t \frac{(t-z)^{\rho-1}\left[F_1(z, \widehat{S}_k(z)) - F_1(z, \widehat{S}_{k-1}(z))\right]}{\Gamma(\rho)} dz \right\| \\ &\leq \frac{1}{\Gamma(\rho)} \int_0^t (t-z)^{\rho-1} \left\| F_1(z, \widehat{S}_k(z)) - F_1(z, \widehat{S}_{k-1}(z)) \right\| dz. \end{aligned}$$

Similarly, for the exposed class

$$\begin{aligned} \|D\widehat{E}_{k+1}(t)\| = \left\|\widehat{E}_{k+1}(t) - \widehat{E}_k(t)\right\| &= \left\| \int_0^t \frac{(t-z)^{\rho-1}\left[F_2(z, \widehat{E}_k(z)) - F_2(z, \widehat{E}_{k-1}(z))\right]}{\Gamma(\rho)} dz \right\| \\ &\leq \int_0^t \frac{(t-z)^{\rho-1} \left\| F_2(z, \widehat{E}_k(z)) - F_2(z, \widehat{E}_{k-1}(z)) \right\|}{\Gamma(\rho)} dz. \end{aligned}$$

Now, for the infected class

$$\|D\widehat{I}_{k+1}(t)\| = \left\|\widehat{I}_{k+1}(t) - \widehat{I}_k(t)\right\| = \left\|\int_0^t \frac{(t-z)^{\rho-1}\left[F_3(z,\widehat{I}_k(z)) - F_3(z,\widehat{I}_{k-1}(z))\right]}{\Gamma(\rho)}dz\right\|$$

$$\leq \frac{1}{\Gamma(\rho)}\int_0^t (t-z)^{\rho-1}\left\|F_3(z,\widehat{I}_k(z)) - F_3(z,\widehat{I}_{k-1}(z))\right\|dz.$$

Lastly, for the recovered class

$$\|D\widehat{R}_{k+1}(t)\| = \left\|\widehat{R}_{k+1}(t) - \widehat{R}_k(t)\right\| = \left\|\int_0^t \frac{(t-z)^{\rho-1}\left[F_4(z,\widehat{R}_k(z)) - F_4(z,\widehat{R}_{k-1}(z))\right]}{\Gamma(\rho)}dz\right\|$$

$$\leq \int_0^t \frac{(t-z)^{\rho-1}\left\|F_4(z,\widehat{R}_k(z)) - F_4(z,\widehat{R}_{k-1}(z))\right\|}{\Gamma(\rho)}dz.$$

Each kernel F_i satisfies the Lipschitz condition with constant κ_i. Thus, each inequality is bounded by a multiple of the norm difference at the previous iteration. Taking the maximum $\sigma = \max\{\kappa_1, \kappa_2, \kappa_3, \kappa_4\} < 1$, we conclude that the sequence is contractive and converges uniformly. Therefore, applying the Banach fixed-point theorem ensures a unique fixed point, confirming that the Mpox model (1.1) possesses a solution. □

Now, we show that the sequence $\{\widehat{S}_n(t)\}$ converges to the exact solution $\widehat{S}(t)$ as $n \to \infty$

$$\left\|\widehat{S}_{n+1}(t) - \widehat{S}(t)\right\| = \left\|\frac{1}{\Gamma(\rho)}\int_0^t (t-z)^{\rho-1}\left[F_1\left(z,\widehat{S}_n(z)\right) - F_1\left(z,\widehat{S}(z)\right)\right]dz\right\|$$

$$\leq \frac{\kappa_1}{\Gamma(\rho)}\int_0^t (t-z)^{\rho-1}\left\|\widehat{S}_n(z) - \widehat{S}(z)\right\|dz$$

Applying iterative estimation and the contraction mapping principle, we obtain

$$\left\|\widehat{S}_{n+1}(t) - \widehat{S}(t)\right\| \leq \left(\frac{\kappa_1 t^\rho}{\Gamma(1+\rho)}\right)^n \left\|\widehat{S}_1(t) - \widehat{S}(t)\right\|,$$

and as $n \to \infty$, it follows that $\widehat{S}_n(t) \to \widehat{S}(t)$ uniformly on $[0,T]$. Similarly, we prove convergence for the other components

$$\left\|\widehat{E}_{n+1}(t) - \widehat{E}(t)\right\| \leq \frac{\kappa_2}{\Gamma(\rho)}\int_0^t (t-z)^{\rho-1}\left\|\widehat{E}_n(z) - \widehat{E}(z)\right\|dz \leq \left(\frac{\kappa_2 t^\rho}{\Gamma(1+\rho)}\right)^n \left\|\widehat{E}_1(t) - \widehat{E}(t)\right\|,$$

$$\left\|\widehat{I}_{n+1}(t) - \widehat{I}(t)\right\| \leq \frac{\kappa_3}{\Gamma(\rho)}\int_0^t (t-z)^{\rho-1}\left\|\widehat{I}_n(z) - \widehat{I}(z)\right\|dz \leq \left(\frac{\kappa_3 t^\rho}{\Gamma(1+\rho)}\right)^n \left\|\widehat{I}_1(t) - \widehat{I}(t)\right\|,$$

$$\left\|\widehat{R}_{n+1}(t)-\widehat{R}(t)\right\| \leq \frac{\kappa_4}{\Gamma(\rho)}\int_0^t (t-z)^{\rho-1}\left\|\widehat{R}_n(z)-\widehat{R}(z)\right\| dz \quad \leq \left(\frac{\kappa_4 t^\rho}{\Gamma(1+\rho)}\right)^n \left\|\widehat{R}_1(t)-\widehat{R}(t)\right\|.$$

Hence, all component sequences converge uniformly to their respective exact solutions. We now demonstrate the uniqueness of solutions for the time-fractional Mpox model.

Theorem 2.3 (Uniqueness of solution)**.** *The fractional-order Mpox model* (1.1) *admits a unique solution if the following condition holds* $\dfrac{\kappa_i t^\rho}{\Gamma(1+\rho)} < 1 \quad$ *for* $i = 1, 2, 3, 4$*, where* κ_i *are the Lipschitz constants corresponding to the kernels* F_i*, and* $\rho \in (0, 1)$ *is the fractional order.*

Proof. Suppose, to the contrary, that there exists another solution $\widehat{S}^\dagger(t), \widehat{E}^\dagger(t), \widehat{I}^\dagger(t), \widehat{R}^\dagger(t)$ to the integral system equivalent to (1.1). Then, according to the definition of a solution of the integral equation, it follows that

$$\begin{cases} \widehat{S}^\dagger(t) = \displaystyle\int_0^t \frac{(t-z)^{\rho-1}F_1(z,\widehat{S}^\dagger(z))}{\Gamma(\rho)}\,dz, \quad \widehat{E}^\dagger(t) = \int_0^t \frac{(t-z)^{\rho-1}F_2(z,\widehat{E}^\dagger(z))}{\Gamma(\rho)}\,dz, \\ \widehat{I}^\dagger(t) = \displaystyle\int_0^t \frac{(t-z)^{\rho-1}F_3(z,\widehat{I}^\dagger(z))}{\Gamma(\rho)}\,dz, \quad \widehat{R}^\dagger(t) = \int_0^t \frac{(t-z)^{\rho-1}F_4(z,\widehat{R}^\dagger(z))}{\Gamma(\rho)}\,dz. \end{cases}$$

Taking norms and using the Lipschitz condition on F_1, we obtain

$$\left\|\widehat{S}(t)-\widehat{S}^\dagger(t)\right\| \leq \frac{1}{\Gamma(\rho)}\int_0^t (t-z)^{\rho-1}\left\|F_1(z,\widehat{S}(z))-F_1(z,\widehat{S}^\dagger(z))\right\| dz \quad \leq \frac{\kappa_1 t^\rho}{\Gamma(1+\rho)}\left\|\widehat{S}(t)-\widehat{S}^\dagger(t)\right\|.$$

If $\kappa_1 t^\rho/\Gamma(1+\rho) < 1$, then it follows that $\left\|\widehat{S}(t)-\widehat{S}^\dagger(t)\right\| = 0$, and hence $\widehat{S}(t) = \widehat{S}^\dagger(t)$.

Proceeding similarly for the remaining components, we obtain

$$\left\|\widehat{E}(t)-\widehat{E}^\dagger(t)\right\| \leq \frac{\kappa_2 t^\rho}{\Gamma(1+\rho)}\left\|\widehat{E}(t)-\widehat{E}^\dagger(t)\right\| \Rightarrow \widehat{E}(t) = \widehat{E}^\dagger(t),$$

$$\left\|\widehat{I}(t)-\widehat{I}^\dagger(t)\right\| \leq \frac{\kappa_3 t^\rho}{\Gamma(1+\rho)}\left\|\widehat{I}(t)-\widehat{I}^\dagger(t)\right\| \Rightarrow \widehat{I}(t) = \widehat{I}^\dagger(t),$$

$$\left\|\widehat{R}(t)-\widehat{R}^\dagger(t)\right\| \leq \frac{\kappa_4 t^\rho}{\Gamma(1+\rho)}\left\|\widehat{R}(t)-\widehat{R}^\dagger(t)\right\| \Rightarrow \widehat{R}(t) = \widehat{R}^\dagger(t).$$

Thus, we conclude that all components of the solution are equal, and the solution to the system is unique. □

3 Stability Analysis of the Solution

Definition 3.1 (Hyers–Ulam stability [9])**.** *The fractional integral system described in* (2.1) *is said to be Hyers–Ulam stable if there exists constants* $\varsigma_i > 0$*,* $i = 1, 2, 3, 4$*, satisfying the following relations for every* $\xi_i > 0$ *such that any functions* $\widehat{S}(t), \widehat{E}(t), \widehat{I}(t), \widehat{R}(t)$ *satisfying*

$$\left|\widehat{S}(t)-\int_0^t\frac{(t-z)^{\rho-1}F_1(z,\widehat{S}(z))}{\Gamma(\rho)}\,dz\right|\leq\xi_1,\quad\left|\widehat{E}(t)-\int_0^t\frac{(t-z)^{\rho-1}F_2(z,\widehat{E}(z))}{\Gamma(\rho)}\,dz\right|\leq\xi_2,$$
$$\left|\widehat{I}(t)-\int_0^t\frac{(t-z)^{\rho-1}F_3(z,\widehat{I}(z))}{\Gamma(\rho)}\,dz\right|\leq\xi_3,\quad\left|\widehat{R}(t)-\int_0^t\frac{(t-z)^{\rho-1}F_4(z,\widehat{R}(z))}{\Gamma(\rho)}\,dz\right|\leq\xi_4.$$

Now, let there exist functions $\widehat{S}^\dagger(t),\widehat{E}^\dagger(t),\widehat{I}^\dagger(t),\widehat{R}^\dagger(t)$ which satisfy the fractional integral system (2.1), that is,

$$\begin{aligned}\widehat{S}^\dagger(t)&=\int_0^t\frac{(t-z)^{\rho-1}}{\Gamma(\rho)}F_1(z,\widehat{S}^\dagger(z))\,dz,\quad\widehat{E}^\dagger(t)&&=\int_0^t\frac{(t-z)^{\rho-1}}{\Gamma(\rho)}F_2(z,\widehat{E}^\dagger(z))\,dz,\\\widehat{I}^\dagger(t)&=\int_0^t\frac{(t-z)^{\rho-1}}{\Gamma(\rho)}F_3(z,\widehat{I}^\dagger(z))\,dz,\quad\widehat{R}^\dagger(t)&&=\int_0^t\frac{(t-z)^{\rho-1}}{\Gamma(\rho)}F_4(z,\widehat{R}^\dagger(z))\,dz.\end{aligned}$$

Then, using the Lipschitz condition of F_1, we find

$$\begin{aligned}\left|\widehat{S}(t)-\widehat{S}^\dagger(t)\right|&=\left|\frac{1}{\Gamma(\rho)}\int_0^t(t-z)^{\rho-1}\left[F_1(z,\widehat{S}(z),\widehat{I}(z))-F_1(z,\widehat{S}^\dagger(z),\widehat{I}(z))\right]\,dz\right|\\&\leq\frac{\kappa_1}{\Gamma(\rho)}\int_0^t(t-z)^{\rho-1}\left|\widehat{S}(z)-\widehat{S}^\dagger(z)\right|\,dz\quad\leq\frac{\kappa_1t^\rho}{\Gamma(1+\rho)}\|\widehat{S}-\widehat{S}^\dagger\|.\end{aligned}$$

Let $\xi_1^\dagger=\dfrac{t^\rho}{\Gamma(1+\rho)}\|\widehat{S}-\widehat{S}^\dagger\|$ and $\varsigma_1=\kappa_1$, so that $\left|\widehat{S}(t)-\widehat{S}^\dagger(t)\right|\leq\xi_1^\dagger\varsigma_1$. Likewise, we derive the following bounds

$$\left|\widehat{E}(t)-\widehat{E}^\dagger(t)\right|\leq\xi_2^\dagger\varsigma_2,\quad\left|\widehat{I}(t)-\widehat{I}^\dagger(t)\right|\leq\xi_3^\dagger\varsigma_3,\quad\left|\widehat{R}(t)-\widehat{R}^\dagger(t)\right|\leq\xi_4^\dagger\varsigma_4.$$

Theorem 3.2 (Hyers-Ulam Stability)**.** *Under the stated assumptions* (C)*, the time-fractional Mpox model* (1.1) *is Hyers-Ulam stable.*

Proof. According to theorem 2.3, the system (1.1) admits a unique solution $\widehat{S}(t),\widehat{E}(t),\widehat{I}(t),\widehat{R}(t)$. Let $\widehat{S}^\dagger(t),\widehat{E}^\dagger(t),\widehat{I}^\dagger(t),\widehat{R}^\dagger(t)$ be any approximate solution to the same system. We begin by estimating the deviation between $\widehat{S}(t)$ and $\widehat{S}^\dagger(t)$

$$\begin{aligned}\left|\widehat{S}(t)-\widehat{S}^\dagger(t)\right|&=\left|\int_0^t\frac{(t-z)^{\rho-1}\left[F_1(z,\widehat{S}(z))-F_1(z,\widehat{S}^\dagger(z))\right]}{\Gamma(\rho)}dz\right|\\&\leq\kappa_1\int_0^t\frac{(t-z)^{\rho-1}\left|\widehat{S}(z)-\widehat{S}^\dagger(z)\right|}{\Gamma(\rho)}dz\leq\frac{\kappa_1t^\rho}{\Gamma(1+\rho)}\left\|\widehat{S}-\widehat{S}^\dagger\right\|.\end{aligned}$$

Define $\kappa_1^\dagger = \dfrac{t^\rho}{\Gamma(1+\rho)}\left\|\widehat{S}-\widehat{S}^\dagger\right\|$, $\varsigma_1^\dagger = \kappa_1$, so we get $\left|\widehat{S}(t)-\widehat{S}^\dagger(t)\right| \leq \kappa_1^\dagger\varsigma_1^\dagger$. Similarly, for the exposed population $\left|\widehat{E}(t)-\widehat{E}^\dagger(t)\right| \leq \dfrac{\kappa_2 t^\rho}{\Gamma(1+\rho)}\left\|\widehat{E}-\widehat{E}^\dagger\right\| = \kappa_2^\dagger\varsigma_2^\dagger$. For the infected population $\left|\widehat{I}(t)-\widehat{I}^\dagger(t)\right| \leq \dfrac{\kappa_3 t^\rho}{\Gamma(1+\rho)}\left\|\widehat{I}-\widehat{I}^\dagger\right\| = \kappa_3^\dagger\varsigma_3^\dagger$ and for the recovered class $\left|\widehat{R}(t)-\widehat{R}^\dagger(t)\right| \leq \dfrac{\kappa_4 t^\rho}{\Gamma(1+\rho)}\left\|\widehat{R}-\widehat{R}\right.$ Thus, all deviations between the true solution and approximate solution are bounded by small multiples of the maximum norm difference, showing Hyers-Ulam-type bounded stability completing the proof. □

4 The Discretized Problem

Let $N \in \mathbb{N}$, and define a uniform time grid over the interval $[0,T]$ as $\{t_j = j\tau : j = 0,1,\ldots,N\}$, where $\tau = T/N$. The Caputo fractional derivative of order $\rho \in (0,1)$ at time t_j for any function $\widehat{X}(t)$ is given by (see, [28])

$$\mathcal{D}_t^\rho \widehat{X}(t_j) = \frac{1}{\Gamma(1-\rho)}\sum_{k=0}^{j-1}\int_{t_k}^{t_{k+1}} (t_j - z)^{-\rho}\widehat{X}'(z)\,dz.$$

$$\begin{aligned}
\mathcal{D}_N^\rho\,\widehat{X}(t_j) &= \frac{1}{\Gamma(1-\rho)}\sum_{k=0}^{j-1}\frac{1}{\tau}\big[\widehat{X}(t_{k+1})-\widehat{X}(t_k)\big]\int_{z=t_k}^{t_{k+1}}(t_j-z)^{-\rho}dz \\
&= \frac{\tau^{-\rho}}{\Gamma(2-\rho)}\sum_{k=0}^{j-1}\big[\widehat{X}(t_{k+1})-\widehat{X}(t_k)\big]d_{j-k} \\
&= \frac{\tau^{-\rho}}{\Gamma(2-\rho)}\Big[\widehat{X}(t_j)d_1 + \sum_{k=1}^{j-1}\big(d_{j-k+1}-d_{j-k}\big)\widehat{X}(t_k) - \widehat{X}(t_0)d_j\Big] \\
&= \frac{1}{\tau^\rho\Gamma(2-\rho)}\sum_{k=0}^{j-1}\Big(\widehat{X}_{k+1}-\widehat{X}_k\Big)\,d_{j-k}
\end{aligned}$$

where the coefficients d_p are defined as $d_p = \dfrac{1}{\tau^\rho\Gamma(2-\rho)}[p^{1-\rho}-(p-1)^{1-\rho}], \quad p = 1,2,\ldots,N.$
Similarly, the L1 discretization of $\mathcal{D}_t^\rho\,\widehat{S}(t), \mathcal{D}_t^\rho\,\widehat{E}(t)$, $\mathcal{D}_t^\rho\,\widehat{I}(t)$ and $\mathcal{D}_t^\rho\,\widehat{R}(t)$ at t_j are

$$\begin{cases}
\mathcal{D}_N^\rho\widehat{S}(t_j) = \displaystyle\sum_{k=0}^{j-1}\Big(\widehat{S}_{k+1}-\widehat{S}_k\Big)\,d_{j-k} + \mathcal{E}_j^{(\widehat{S})}, & \mathcal{D}_N^\rho\widehat{E}(t_j) = \displaystyle\sum_{k=0}^{j-1}\Big(\widehat{E}_{k+1}-\widehat{E}_k\Big)\,d_{j-k} + \mathcal{E}_j^{(\widehat{E})}, \\
\mathcal{D}_N^\rho\widehat{I}(t_j) = \displaystyle\sum_{k=0}^{j-1}\Big(\widehat{I}_{k+1}-\widehat{I}_k\Big)\,d_{j-k} + \mathcal{E}_j^{(\widehat{I})}, & \mathcal{D}_N^\rho\widehat{R}(t_j) = \displaystyle\sum_{k=0}^{j-1}\Big(\widehat{R}_{k+1}-\widehat{R}_k\Big)\,d_{j-k} + \mathcal{E}_j^{(\widehat{R})}.
\end{cases}$$

where $\mathcal{E}_j^{(\widehat{S})}, \mathcal{E}_j^{(\widehat{E})}, \mathcal{E}_j^{(\widehat{I})}, \mathcal{E}_j^{(\widehat{R})}$ denote the local truncation errors at t_j associated with each

equation. Neglecting the error term, Substituting these approximation into the Mpox model (1.1), we obtain the discretized system

$$\begin{cases} \mathcal{D}_N^\rho \widehat{S}(t_j) = \Lambda - \beta \widehat{S}_j \widehat{I}_j - (\nu+\mu)\widehat{S}_j, \quad \mathcal{D}_N^\rho \widehat{E}(t_j) = \beta \widehat{S}_j \widehat{I}_j - (\gamma+\mu)\widehat{E}_j, \\ \mathcal{D}_N^\rho \widehat{I}(t_j) = \gamma \widehat{E}_j - (\alpha+\sigma+\mu)\widehat{I}_j, \quad \mathcal{D}_N^\rho \widehat{R}(t_j) = \nu \widehat{S}_j + \alpha \widehat{I}_j - \mu \widehat{R}_j \end{cases} \tag{4.1}$$

after simplification, the L1-discretized system (4.1) yields the following nonlinear algebraic equations at each time step t_j

$$\begin{cases} (d_1+\nu+\mu)\,\widehat{S}_j + \beta \widehat{S}_j \widehat{I}_j - \Lambda + \sum_{k=1}^{j-1}(d_{j-k+1}-d_{j-k})\widehat{S}_k - \widehat{S}_0 d_j = 0, \\ (d_1+\mu+\gamma)\,\widehat{E}_j - \beta \widehat{S}_j \widehat{I}_j + \sum_{k=1}^{j-1}(d_{j-k+1}-d_{j-k})\widehat{E}_k - \widehat{E}_0 d_j = 0, \\ (d_1+\mu+\sigma+\alpha)\,\widehat{I}_j - \gamma \widehat{E}_j + \sum_{k=1}^{j-1}(d_{j-k+1}-d_{j-k})\widehat{I}_k - \widehat{I}_0 d_j = 0, \\ (d_1+\mu)\,\widehat{R}_j - \nu \widehat{S}_j - \alpha \widehat{I}_j + \sum_{k=1}^{j-1}(d_{j-k+1}-d_{j-k})\widehat{R}_k - \widehat{R}_0 d_j = 0, \end{cases} \tag{4.2}$$

for $j = 1, 2, \ldots, N$, where $\widehat{S}_j = \widehat{S}(t_j)$ similary for $\widehat{E}_j, \widehat{I}_j, \widehat{R}_j$. We define the nonlinear system compactly as

$$\begin{cases} f_1(\widehat{S}_j, \widehat{E}_j, \widehat{I}_j, \widehat{R}_j) = 0, f_2(\widehat{S}_j, \widehat{E}_j, \widehat{I}_j, \widehat{R}_j) &= 0, \\ f_3(\widehat{S}_j, \widehat{E}_j, \widehat{I}_j, \widehat{R}_j) = 0, f_4(\widehat{S}_j, \widehat{E}_j, \widehat{I}_j, \widehat{R}_j) &= 0, \end{cases} \tag{4.3}$$

with $\widehat{S}_j, \widehat{E}_j, \widehat{I}_j, \widehat{R}_j \geq 0$. This nonlinear system is solved iteratively using the Newton–Raphson method. Let the initial guess at time t_j be $[\widehat{S}_j^{(0)}, \widehat{E}_j^{(0)}, \widehat{I}_j^{(0)}, \widehat{R}_j^{(0)}]$, at the n^{th} iteration is

$$\begin{bmatrix} \widehat{S}_j^{(n)} \\ \widehat{E}_j^{(n)} \\ \widehat{I}_j^{(n)} \\ \widehat{R}_j^{(n)} \end{bmatrix} = \begin{bmatrix} \widehat{S}_j^{(n-1)} \\ \widehat{E}_j^{(n-1)} \\ \widehat{I}_j^{(n-1)} \\ \widehat{R}_j^{(n-1)} \end{bmatrix} - J_{n-1}^{-1} \begin{bmatrix} f_1(\widehat{S}_j^{(n-1)}, \widehat{E}_j^{(n-1)}, \widehat{I}_j^{(n-1)}, \widehat{R}_j^{(n-1)}) \\ f_2(\widehat{S}_j^{(n-1)}, \widehat{E}_j^{(n-1)}, \widehat{I}_j^{(n-1)}, \widehat{R}_j^{(n-1)}) \\ f_3(\widehat{S}_j^{(n-1)}, \widehat{E}_j^{(n-1)}, \widehat{I}_j^{(n-1)}, \widehat{R}_j^{(n-1)}) \\ f_4(\widehat{S}_j^{(n-1)}, \widehat{E}_j^{(n-1)}, \widehat{I}_j^{(n-1)}, \widehat{R}_j^{(n-1)}) \end{bmatrix},$$

where J_{n-1} is the Jacobian matrix evaluated at the previous iteration. This procedure is repeated at each time step j, thereby solving the entire time-fractional Mpox system. The Jacobian matrix $J_{(p)}$ of the nonlinear system at the p^{th} iteration is given by

$$J_{(p)} = \left[\begin{array}{cccc} \dfrac{\partial f_1}{\partial \widehat{S}} & \dfrac{\partial f_1}{\partial \widehat{E}} & \dfrac{\partial f_1}{\partial \widehat{I}} & \dfrac{\partial f_1}{\partial \widehat{R}} \\ \dfrac{\partial f_2}{\partial \widehat{S}} & \dfrac{\partial f_2}{\partial \widehat{E}} & \dfrac{\partial f_2}{\partial \widehat{I}} & \dfrac{\partial f_2}{\partial \widehat{R}} \\ \dfrac{\partial f_3}{\partial \widehat{S}} & \dfrac{\partial f_3}{\partial \widehat{E}} & \dfrac{\partial f_3}{\partial \widehat{I}} & \dfrac{\partial f_3}{\partial \widehat{R}} \\ \dfrac{\partial f_4}{\partial \widehat{S}} & \dfrac{\partial f_4}{\partial \widehat{E}} & \dfrac{\partial f_4}{\partial \widehat{I}} & \dfrac{\partial f_4}{\partial \widehat{R}} \end{array} \right]_{(\widehat{S},\widehat{E},\widehat{I},\widehat{R})=(\widehat{S}^{(p)}(t_j),\widehat{E}^{(p)}(t_j),\widehat{I}^{(p)}(t_j),\widehat{R}^{(p)}(t_j))}.$$

Then, the approximate solution of system (1.1) at time step t_j, after n iterations, is given by

$$\begin{bmatrix} \widehat{S}(t_j) \\ \widehat{E}(t_j) \\ \widehat{I}(t_j) \\ \widehat{R}(t_j) \end{bmatrix} \approx \begin{bmatrix} \widehat{S}^{(n)}(t_j) \\ \widehat{E}^{(n)}(t_j) \\ \widehat{I}^{(n)}(t_j) \\ \widehat{R}^{(n)}(t_j) \end{bmatrix}.$$

5 Error Analysis

In this section, we present a rigorous error analysis of the L1 scheme applied to the time-fractional Mpox model (1.1). We assume that the exact solution $\widehat{Z}(t) = [\widehat{S}(t), \widehat{E}(t), \widehat{I}(t), \widehat{R}(t)]^\top \in \mathcal{C}^2[0,T]$ satisfies the following regularity condition [4, 23]

$$\left\| \frac{d^p \widehat{Z}(t)}{dt^p} \right\| \leq C(1 + t^{\rho - p}), \quad \text{for } p = 0, 1, 2. \tag{5.1}$$

This condition accounts for the weak singularity at $t = 0$, since $\widehat{Z}'(t) \sim t^{\rho-1} \to \infty$ as $t \to 0^+$.

Theorem 5.1 (Local Truncation Error)**.** *Let $\widehat{Z}(t)$ satisfy the regularity assumption* (5.1)*. Then, the L1 approximation to the Caputo derivative satisfies*

$$\left\| \mathcal{D}_t^\rho \widehat{Z}(t_j) - \mathcal{D}_N^\rho \widehat{Z}(t_j) \right\| \leq C\, N^{-\rho} \quad \textit{for } j = 1, 2, \ldots, N.$$

Proof. Following the L1 truncation analysis framework in [23], the local error in approximating the Caputo derivative by the L1 formula is given by

$$\mathcal{E}_j^{(X)} = \mathcal{D}_t^\rho \widehat{X}(t_j) - \mathcal{D}_N^\rho \widehat{X}(t_j), \quad \widehat{X} \in \{\widehat{S}, \widehat{E}, \widehat{I}, \widehat{R}\}.$$

Each term involves integrals of the form

$$T_{jk} = \int_{t_k}^{t_{k+1}} (t_j - s)^{-\rho} \left(\frac{d\widehat{X}(s)}{ds} - \delta_k \right) ds,$$

where δ_k denotes the piecewise linear interpolant of $\widehat{X}$ over $[t_k, t_{k+1}]$. Using Taylor expansion and the regularity condition (5.1), we estimate

$$|T_{jk}| \leq C\tau_{k+1} \int_{t_k}^{t_{k+1}} (t_j - s)^{-\rho}(s - t_k)ds \leq C\tau_{k+1}^2 (t_j - t_k)^{-\rho}.$$

Summing over all k, and applying mesh-dependent bounds, we obtain $|\mathcal{E}_j^{(X)}| \leq \sum_{k=0}^{j-1} |T_{jk}| \leq C\, N^{-\rho}$. □

Let the error vector at time t_j be defined as

$$\mathcal{E}_j = \widehat{Z}(t_j) - \widehat{Z}_j = \begin{bmatrix} \widehat{S}(t_j) - \widehat{S}_j \\ \widehat{E}(t_j) - \widehat{E}_j \\ \widehat{I}(t_j) - \widehat{I}_j \\ \widehat{R}(t_j) - \widehat{R}_j \end{bmatrix}.$$

Subtracting the numerical scheme (4.2) from the continuous model (1.1), and applying the L1 discretization gives $\mathcal{D}_N^\rho \mathcal{E}_j = F(t_j, \widehat{Z}(t_j)) - F(t_j, \widehat{Z}_j) + \mathcal{T}_j$, where $\mathcal{T}_j = [\mathcal{D}_t^\rho \widehat{Z}(t_j) - \mathcal{D}_N^\rho \widehat{Z}(t_j)]$ denotes the truncation error vector.

Theorem 5.2 (Stability)**.** *Assume that the function $F(t, \widehat{Z})$ satisfies a global Lipschitz condition in $\widehat{Z}$. Then the error satisfies*

$$\|\mathcal{E}_j\| \leq C \sup_{1 \leq k \leq j-1} \|\mathcal{T}_k\|, \quad \textit{for } j \geq 1.$$

Proof. Using the Lipschitz continuity of F, we write $\mathcal{D}_N^\rho \|\mathcal{E}_j\| \leq L\|\mathcal{E}_j\| + \|\mathcal{T}_j\|$. In the discrete L1 formulation, the inequality can be expressed in the form

$$d_{j,j-1}\|\mathcal{E}_j\| - \sum_{k=1}^{j-1} \big(d_{j,k} - d_{j,k-1}\big)\|\mathcal{E}_k\| \leq L\|\mathcal{E}_j\| + \|\mathcal{T}_j\|,$$

Rearranging, we obtain

$$\Big(\frac{\tau_j^{-\rho}}{\Gamma(2-\rho)} - L\Big)\|\mathcal{E}_j\| \leq M \sum_{k=1}^{j-1} \|\mathcal{E}_k\| + \|\mathcal{T}_j\|,$$

where $M = \max_{1 \leq k \leq j-1} \{d_{j,k} - d_{j,k-1}\}$. From [12], provided $L\Gamma(2-\rho) < \tau_j^{-\rho}$ and $\lim_{h \to 0} \sum_{k=1}^{j-1} \|\mathcal{E}_k\| = 0$, the discrete fractional Grönwall inequality ensures $\|\mathcal{E}_j\| \leq C \sup_{1 \leq k \leq j-1} \|\mathcal{T}_k\|$. Hence, the desired stability bound is obtained. □

Theorem 5.3 (Global Convergence)**.** *Suppose the regularity assumption* (5.1) *holds, and that $F(t, \widehat{Z})$ is Lipschitz continuous. Then, the L1 scheme satisfies the following global error estimate*

$$\max_{1 \leq j \leq N} \|\widehat{Z}(t_j) - \widehat{Z}_j\| \leq C\, N^{-\rho}.$$

Proof. Combining Lemma 5.1 and Theorem 5.2, we obtain, $\|\mathcal{E}_j\| \leq C \sup_{1\leq k\leq j-1} \|\mathcal{T}_k\| \leq C\, N^{-\rho}$. □

6 Numerical illustration and discussions

To validate the accuracy and efficiency of the proposed scheme, the following test example is considered. The corresponding order of convergence is calculated by $\varrho_M = \log_2\left(\Sigma_M/\Sigma_{2M}\right)$, and the maximum errors are calculated by $\Sigma_M = \max_{0\leq j\leq M} \left|U(y_j) - U_j\right|$.All computations are performed using MATLAB R2016a.

Example 6.1. *Consider the fractional-order Mpox model* (1.1) *with the following initial conditions and parameter values adapted from [1],*

$$\Lambda = 0.01630, \quad \beta = 0.050, \quad \mu = 0.00910, \quad \nu \in [0, 1],$$
$$\gamma = 0.05882, \quad \alpha = 0.06125, \quad \sigma = 0.0300,$$
$$\widehat{S}(0) = 0.90, \quad \widehat{E}(0) = 0.06, \quad \widehat{I}(0) = 0.04, \quad \widehat{R}(0) = 0.$$

To validate the L1 scheme, numerical simulations are performed for various values of the fractional order $\rho \in \{0.80, 0.90, 0.95, 0.99\}$. A refined solution computed on a mesh of size $2M$ is taken as the reference to evaluate the error on a coarse mesh of size M. The maximum absolute errors between the coarse and refined solutions are computed for each compartment ($\widehat{S}$, $\widehat{E}$, $\widehat{I}$, and $\widehat{R}$). The results, as shown in table [2 - 5], demonstrate that the L1 scheme achieves high accuracy, particularly for higher values of ρ.

Log-log plots of the numerical errors with respect to mesh size M confirm that the L1 scheme exhibits algebraic convergence with rate close to $\mathcal{O}(M^{-\rho})$ for all compartments. These results are depicted in figure 4.The observed rates match the theoretical prediction, validating the consistency of the scheme.

Figures 1 and 2 show the time evolution of each compartment for different values of ρ. The results reveal that, As ρ increases, the susceptible population $\widehat{S}$ decays faster, while the exposed and infected populations rise earlier and decline faster, suggesting more substantial memory effects. For lower ρ, the infection process is more delayed, reflecting the fractional derivative's non-local nature and the presence of memory in disease progression. The recovered class $\widehat{R}$ increases more slowly for lower ρ, indicating that the fractional order significantly influences the pace of recovery in the population.

The effect of varying vaccination rate $\nu \in \{0, 0.2, 0.5\}$ is examined in Figures 3 . An increase in vaccination rate leads to a significant reduction in the peak and size of both the exposed and infected populations. This supports the effectiveness of vaccination strategies in controlling the Mpox outbreak.

A comparative study between the L1 scheme and the FMEM is conducted. The results table 6 reveals that the L1 scheme significantly outperforms FMEM in terms of accuracy for all values of ρ. These findings confirm the robustness, convergence, and computational advantage of the L1 scheme in solving the time-fractional Mpox model.

Table 2: $\mathcal{E}_M^N$ *and* ϱ_M^N *of* $\widehat{S}$ *for Example 6*

ρ	32	64	128	256	512	1024
0.10	7.276E-03	6.941E-03	6.612E-03	6.291E-03	5.979E-03	5.677E-03
	0.068	0.070	0.072	0.073	0.075	0.076
0.30	1.808E-02	1.555E-02	1.325E-02	1.119E-02	9.392E-03	7.835E-03
	0.217	0.231	0.243	0.253	0.262	0.268
0.50	2.469E-02	1.881E-02	1.402E-02	1.028E-02	7.457E-03	5.367E-03
	0.392	0.424	0.447	0.463	0.475	0.482
0.70	2.794E-02	1.816E-02	1.151E-02	7.334E-03	4.580E-03	2.834E-03
	0.622	0.658	0.650	0.679	0.692	0.698
0.90	3.092E-02	1.848E-02	1.039E-02	5.627E-03	2.985E-03	1.569E-03
	0.743	0.831	0.885	0.915	0.928	0.932

Table 3: $\mathcal{E}_M^N$ *and* ϱ_M^N *of* $\widehat{E}$ *for Example 6*

ρ	32	64	128	256	512	1024
0.20	3.913E-04	3.432E-04	3.007E-04	2.632E-04	2.301E-04	2.011E-04
	0.189	0.191	0.192	0.194	0.195	0.195
0.40	6.221E-04	4.762E-04	3.634E-04	2.768E-04	2.105E-04	1.599E-04
	0.385	0.390	0.393	0.395	0.396	0.397
0.60	7.017E-04	4.625E-04	3.047E-04	2.008E-04	1.325E-04	8.738E-05
	0.601	0.602	0.601	0.601	0.600	0.600
0.80	8.024E-04	4.541E-04	2.522E-04	1.398E-04	7.827E-05	4.439E-05
	0.821	0.849	0.851	0.837	0.818	0.808
0.99	1.114E-03	6.044E-04	3.159E-04	1.617E-04	8.184E-05	4.116E-05
	0.883	0.936	0.966	0.983	0.992	0.996

Table 4: $\mathcal{E}_M^N$ *and* ϱ_M^N *of* $\widehat{I}$ *for Example 6*

ρ	32	64	128	256	512	1024
0.10	4.600E-05	4.552E-05	4.480E-05	4.386E-05	4.275E-05	4.151E-05
	0.015	0.023	0.031	0.037	0.043	0.047
0.30	1.214E-04	1.131E-04	1.019E-04	8.967E-05	7.751E-05	6.612E-05
	0.102	0.151	0.185	0.210	0.229	0.244
0.50	1.863E-04	1.530E-04	1.189E-04	8.941E-05	6.588E-05	4.791E-05
	0.284	0.364	0.411	0.441	0.460	0.472
0.80	3.336E-04	1.958E-04	1.108E-04	6.206E-05	3.446E-05	1.924E-05
	0.769	0.821	0.837	0.849	0.841	0.829
0.90	5.265E-04	2.768E-04	1.415E-04	7.123E-05	3.564E-05	1.779E-05
	0.928	0.968	0.990	0.999	1.002	1.003

Table 5: $\mathcal{E}_M^N$ *and* ϱ_M^N *of* $\widehat{R}$ *for Example 6*

ρ	32	64	128	256	512	1024
0.20	1.514E-02	1.366E-02	1.228E-02	1.100E-02	9.819E-03	8.741E-03
	0.148	0.154	0.159	0.164	0.168	0.172
0.40	2.479E-02	1.996E-02	1.586E-02	1.246E-02	9.709E-03	7.516E-03
	0.313	0.332	0.348	0.360	0.369	0.377
0.60	2.984E-02	2.098E-02	1.438E-02	9.700E-03	6.483E-03	4.310E-03
	0.508	0.545	0.568	0.581	0.589	0.593
0.70	3.085E-02	1.993E-02	1.270E-02	8.067E-03	5.030E-03	3.111E-03
	0.630	0.650	0.655	0.681	0.693	0.698
0.99	3.438E-02	1.971E-02	1.081E-02	5.675E-03	2.912E-03	1.477E-03
	0.803	0.867	0.929	0.962	0.979	0.988

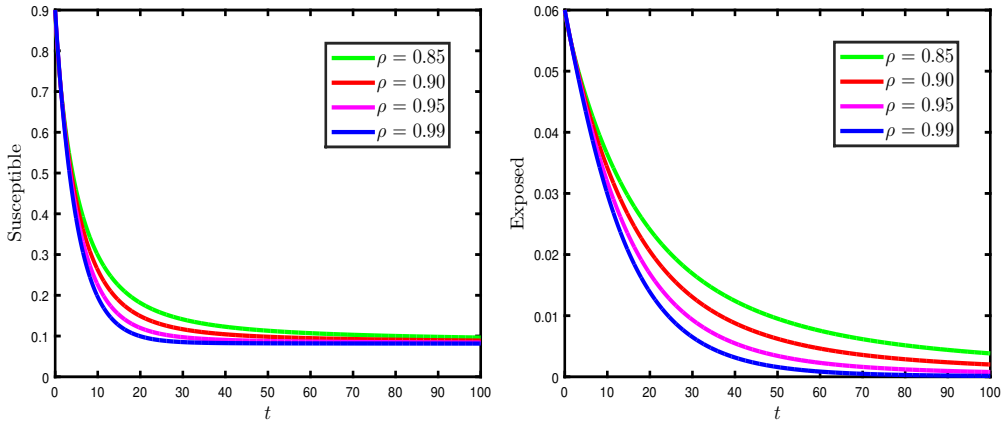

Figure 1: Comparison of $\widehat{S}(t)$ and $\widehat{E}(t)$ for different values of ρ

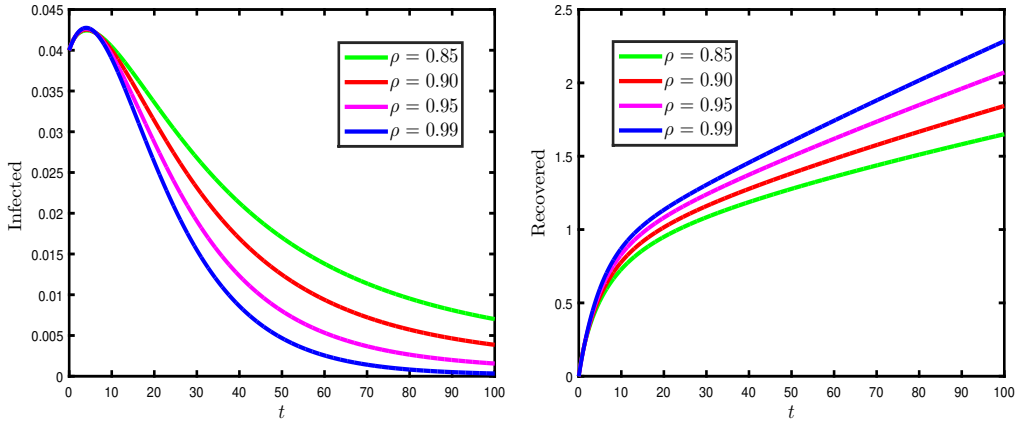

Figure 2: Comparison of $\widehat{I}(t)$ and $\widehat{R}(t)$ for different values of ρ

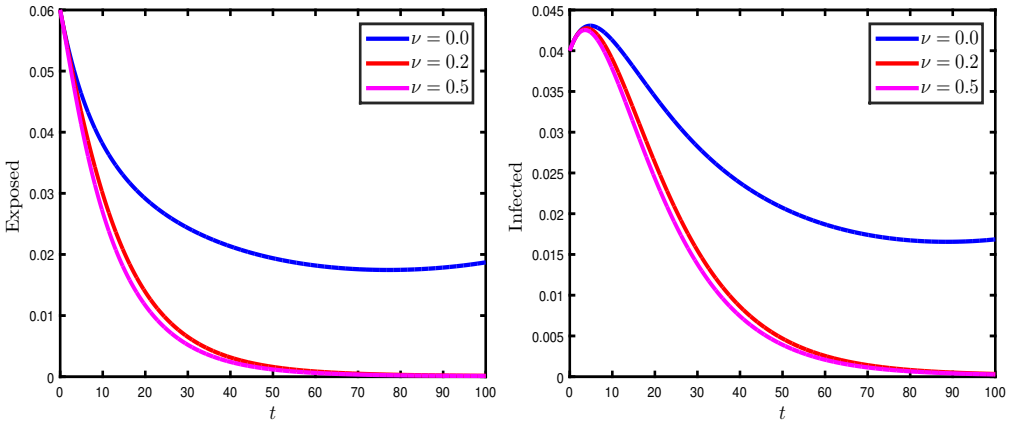

Figure 3: Effect of vaccination rate on $\widehat{E}(t)$ and $\widehat{I}(t)$

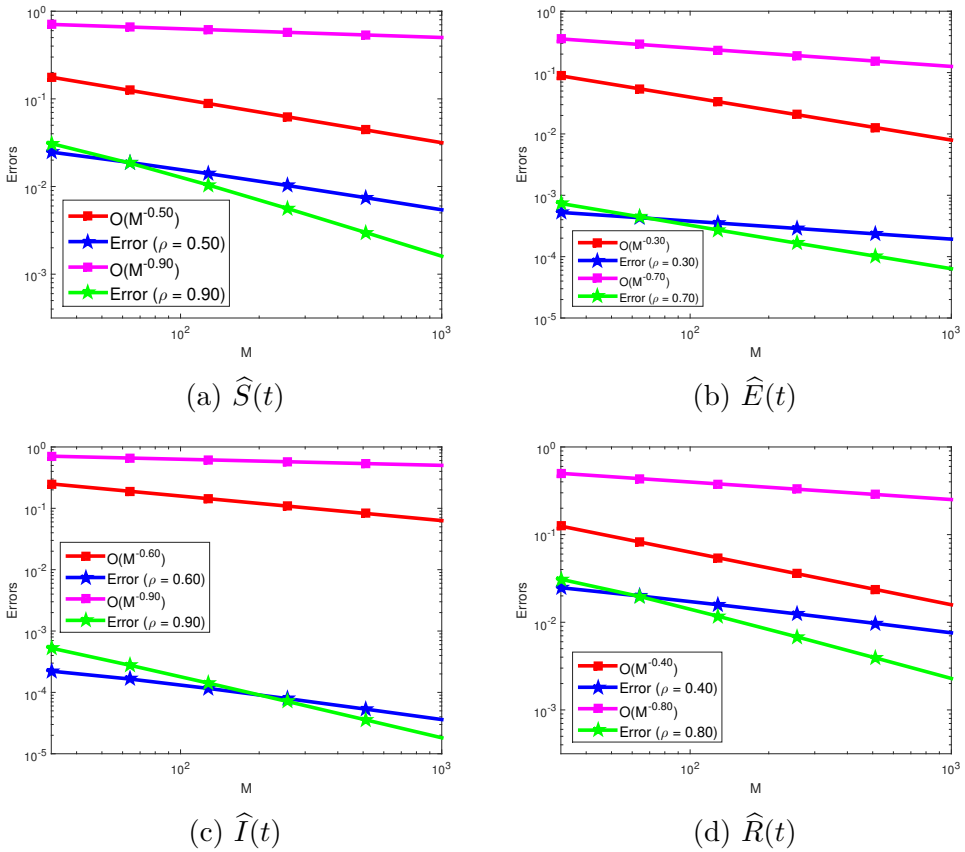

(a) $\widehat{S}(t)$ (b) $\widehat{E}(t)$

(c) $\widehat{I}(t)$ (d) $\widehat{R}(t)$

Figure 4: Log-log plots for Example 6

Table 6: Comparison of maximum absolute errors using L1 and FMEM schemes [1] for compartments $\widehat{S}$, $\widehat{E}$, $\widehat{I}$, and $\widehat{R}$ at different values of ρ.

ρ	$\widehat{S}$		$\widehat{E}$		$\widehat{I}$		$\widehat{R}$	
	L1	FMEM	L1	FMEM	L1	FMEM	L1	FMEM
0.80	8.57E–4	3.78E–2	1.87E–5	3.44E–3	7.92E–6	3.99E–3	9.40E–4	3.90E–1
0.90	5.76E–4	1.89E–2	1.32E–5	1.72E–3	6.06E–6	2.00E–3	6.25E–4	1.40E–1
0.95	5.15E–4	9.47E–3	1.32E–5	8.62E–4	7.75E–6	1.00E–3	5.45E–4	5.84E–2
0.99	5.06E–4	1.89E–3	1.41E–5	1.72E–4	9.90E–6	2.00E–4	5.10E–4	1.00E–2

7 Conclusion

In this study, we proposed and analyzed a fractional-order mathematical model for the Mpox virus. We examined the model existence, uniqueness, and stability properties and solved it numerically using the L1 scheme with Newton–Raphson iteration. A thorough error analysis was carried out, demonstrating that the L1 scheme exhibits convergence aligning well with theoretical predictions. Initial conditions and parameters were taken from existing literature to simulate disease dynamics.Using the Caputo derivative, we explored the impact of different fractional orders and vaccination rates on disease progression. The L1 scheme demonstrated high accuracy in all compartments. This underscores the significance of fractional calculus in modeling infectious diseases like Mpox.

Conflicts of interest

The authors declare that there are no conflicts of interest.

Funding

Not Applicable

References

[1] I. M. Batiha, A. A. Abubaker, I. H. Jebril, S. B. Al-Shaikh, K. Matarneh and M. Almuzini, A mathematical study on a fractional-order SEIR Mpox model: analysis and vaccination influence, Algorithms, **16**(9) (2023), 418.

[2] C. Benzarouala, C. Tunç, *Hyers–Ulam–Rassias stability of fractional delay differential equations with Caputo derivative*, Math. Methods Appl. Sci., **47**(18)(2024), 13499-13509.

[3] Centers for Disease Control and Prevention, *Monkeypox: Clinical Recognition*, CDC Public Health Guidance (2022). Available at: `https://www.cdc.gov/mpox/hcp/clinical-signs/?CDC_AAref_Val=https://www.cdc.gov/poxvirus/mpox/clinicians/clinical-recognition.html`

[4] K. Diethelm, The Analysis of Fractional Differential Equations: An Application-Oriented Exposition Using Differential Operators of Caputo Type, Springer, Berlin, 2010.

[5] A. Elsonbaty, W. Adel, A. Aldurayhim and A. El-Mesady, *Mathematical modeling and analysis of a novel monkeypox virus spread integrating imperfect vaccination and non-linear incidence rates*, Ain Shams Eng. J., **15**(3) (2024), 102451.

[6] H. Fallahgoul, S. Focardi and F. Fabozzi, *Fractional Calculus and Fractional Processes with Applications to Financial Economics: Theory and Application*, Academic Press, 2016.

[7] B. Ghosh and J. Mohapatra, *Numerical simulation for two species time fractional weakly singular model arising in population dynamics*, Int. J. Model. Simul. (2023), 1–14.

[8] M. Helikumi, F. Ojija and A. Mhlanga, *Dynamical Analysis of Mpox Disease with Environmental Effects*, Fractal and Fractional, **9**(6) (2025), 356.

[9] S. M. Jung, *Hyers-Ulam stability of linear differential equations of first order*, Appl. Math. Lett., **17**(10) (2004), 1135–1140.

[10] A. A. Kilbas, Theory and Applications of Fractional Differential Equations, *North-Holland Mathematics Studies*, New York, 2006.

[11] P. Kumar, M. Vellappandi, Z. A. Khan, S. SM, A. Kaziboni and V. Govindaraj, *A case study of monkeypox disease in the United States using mathematical modeling with real data*, Math. Comput. Simul., **213** (2023), 444–465.

[12] P. Linz, *Analytical and Numerical Methods for Volterra Equations*, SIAM, Philadelphia, 1985.

[13] S. Majee, S. Jana, S. Barman and T. K. Kar, *Transmission dynamics of monkeypox virus with treatment and vaccination controls: a fractional order mathematical approach*, Physica Scripta, **98**(2) (2023), 024002.

[14] M. Manivel, A. Venkatesh, K. A. Kumar, M. P. Raj, S. E. Fadugba and M. Kekana, *Quantitative modeling of monkeypox viral transmission using Caputo fractional variational iteration method*, Partial Differ. Equ. Appl. Math., **13** (2025), 101026.

[15] F. Mainardi, *Fractional Calculus and Waves in Linear Viscoelasticity*, World Scientific, 2022.

[16] G. Saini, B. Ghosh, S. Chand, *An accurate computational approach for solving system of differential equations involving non-local derivatives*, J. Math. Model., (2025).

[17] S. Paul, A. Mahata, M. Karak, S. Mukherjee, S. Biswas and B. Roy, *Dynamical behavior of fractal-fractional order monkeypox virus model*, Franklin Open, **7** (2024), 100103.

[18] O. J. Peter, F. A. Oguntolu, M. M. Ojo, A. O. Oyeniyi, R. Jan and I. Khan, Fractional order mathematical model of monkeypox transmission dynamics, Physica Scripta, **97**(8) (2022), 084005.

[19] I. Podlubny, Fractional differential equations, mathematics in science and engineering, *Academic press New York* 1999.

[20] M. U. Rahman, Y. Karaca, R. P. Agarwal and S. Adriani David, *Mathematical modelling with computational fractional order for the unfolding dynamics of the communicable diseases*, Appl. Math. Sci. Eng., **32**(1) (2024), 2300330.

[21] N. Raji Reddy, J. Mohapatra, A robust numerical scheme for singularly perturbed delay parabolic initial-boundary-value problems involving mixed space shifts. Comput. Methods Differ. Equ., **11** (1)(2023) 42-51.

[22] S. Ramzan, S. A. Zanib, M. A. Shah, N. Abbas and W. Shatanawi, *Analytical study of a modified monkeypox virus model using Caputo–Fabrizio fractional derivatives*, Model. Earth Syst. Environ., **10**(5) (2024), 6475–6492.

[23] M. Stynes, E. O'Riordan and J. L. Gracia, *Error analysis of a finite difference method on graded meshes for a time-fractional diffusion equation*, SIAM J. Numer. Anal., **55**(2) (2017), 1057–1079.

[24] C. Tunç, O. Tunç, *Ulam-type stability of $\psi-$ Hilfer fractional-order integro-differential equations with multiple variable delays*, Asian J. Control (2025) https://doi.org/10.1002/asjc.3645.

[25] O. Tunç, C. Tunç, *On Ulam stabilities of iterative Fredholm and Volterra integral equations with multiple time-varying delays*, Rev. Real Acad. Cienc. Exactas Fis. Nat. Ser. A-Mat. **118**(3) (2024), 83.

[26] O. Tunç, C. Tunç, G. Petruşel,J. C. Yao, *On the Ulam stabilities of nonlinear integral equations and integro-differential equations*, Math. Methods Appl. Sci., **47**(6) (2024), 4014-4028.

[27] X. J Yang, F. Gao and Y. Ju, *General Fractional Derivatives with Applications in Viscoelasticity*, Academic Press, 2020.

[28] Y. Lin and C. Xu, Finite difference/spectral approximations for the time-fractional diffusion equation, *J. Comput. Phys.* **225**(2) (2007), 1533–1552.

[29] H. Zhao, L. Wang, S. M. Oliva and H. Zhu, *Modeling and dynamics analysis of Zika transmission with limited medical resources*, Bull. Math. Biol., **82**(8) (2020), 99.